Properties of the tip-plane configuration

1971 J. Phys. D: Appl. Phys. 4 1266

(http://iopscience.iop.org/0022-3727/4/9/305)

J. Phys. D: Appl. Phys., 1971, Vol. 4. Printed in Great Britain

Properties of the tip–plane configuration

R. COELHO† and J. DEBEAU‡

† Laboratoire de Génie Electrique de la Faculté des Sciences de Paris, 33 Avenue du Général Leclerc, 92-Fontenay-aux-Roses, Paris, France
‡ Laboratoire Central des Industries Electriques de la Faculté des Sciences de Paris, 33 Avenue du Général Leclerc, 92-Fontenay-aux-Roses, Paris, France

MS. received 29th December 1970

Abstract. Electrostatic properties of the point–plane electrode configuration are reviewed in the hyperbolic approximation. Simple expressions for the field in the neighbourhood of the tip are derived under the assumption that space-charge distortion is absent. Current induced by a charge carrier moving along a field line is investigated and the theoretical expressions are compared with experimental results. Finally, the problem of the space charge is solved along the tip axis.

1. Introduction

A great many investigations in dielectric conduction and breakdown (Nikolopoulos 1966, Coelho and Sibillot 1970 a), field emission and field ion microscopy (Gomer 1961, Drechsler and Henkel 1964) and electrochemistry make use of the point–plane electrode configuration with its strongly divergent electric field.

Apart from the divergence itself, which may be used for example in dielectrophoretic separation, another feature of point–plane configurations is that a reasonably low applied voltage V may produce a huge electric field E at the point apex. The widely used approximation $E_{tip} \simeq V/5r$, where r is the radius of curvature at the apex, shows that with a relatively sharp tip (say $r=1$ μm) and a voltage of, say, 1 kV the magnitude of the apex fields is 2×10^6 V cm^{-1}.

In this paper we discuss the validity of the approximation mentioned above; then, after considering briefly the motion of a free charge in an empty point–plane configuration, we discuss the motion of a charge along the field lines in a space-charge-free medium, where the charge carriers are characterized by a mobility μ, and calculate transfer times.

Finally, we take up the problem of the space-charge self-consistent field along the axis.

Wherever possible, we compare the results with experimental data.

2. Derivation of the applied field

2.1. *The approximation*

In order to calculate the electric field in the point–plane gap, one must first adopt a simple geometric approximation. Perhaps the simplest of these is the paraboloid approximation, which has been discussed by Nikolopoulos (1966). However, the profile of actual points does not fit the shape of a paraboloid, unless the tip radius is rather large. Drechsler and Henkel (1964) used a half sphere on a truncated cone. This approximation is likely to fit actual tip shapes better, since two independent parameters are involved herein (tip radius and shaft angle), but its relative analytical complexity prevents any analysis much more detailed than the evaluation of the field along the tip axis, especially if space charge is taken into account.

Consequently, we shall use here the hyperboloid approximation, which also involves two parameters and has already been studied by Durand (1966). Using Durand's notations,

the tip is generated by the hyperbola of equations

$$\begin{aligned} x &= a \sin \zeta \cosh \eta \\ y &= a \cos \zeta \sinh \eta \end{aligned} \tag{1}$$

rotating around the x axis.

Equations (1) define two orthogonal confocal sets of ellipses and hyperbolas. Since we consider the hyperbolas only, ζ must be regarded as the parameter defining the hyperbola. Particular values of ζ are

$\zeta = 0$	$(x=0)$	Oy axis generating the plane
$\zeta = \pi/2$	$(y=0)$	Ox axis generating an infinitely sharp hyperbola.

η is the parameter defining a particular point on the hyperbola defined by ζ.

It is shown in Durand's book that if two of the hyperbolas are equipotential surfaces all of the hyperbolas of the set are also equipotentials and, furthermore, that if the origin of the potential is taken at the plane $x=0$ ($\zeta=0$) the potential $V(\zeta)$ of the hyperbola of parameter ζ is

$$V(\zeta) = C \ln \tan (\zeta/2 + \pi/4) \tag{2}$$

where C is a constant depending on the applied voltage. The flux lines of the field generate a family of ellipsoids of revolution orthogonal to the hyperboloids, and the value of the electric field at point (ζ, η) is

$$E(\zeta, \eta) = \frac{C}{a \cos \zeta (\cosh^2 \eta - \sin^2 \zeta)^{1/2}}. \tag{3}$$

The constant C is calculated as follows: under the assumption that the point is sharp, the corresponding value of ζ is close to $\pi/2$. If V is the potential of the point, we have $V(\pi/2 - \epsilon) = V$, with $\epsilon \ll 1$, so that, using (2),

$$V = C \ln \tan \left(\frac{\pi}{2} - \frac{\epsilon}{2} \right) = C \ln \cot \frac{\epsilon}{2}$$

or

$$V = C \ln \left(\frac{2}{\epsilon} - \frac{\epsilon}{6} + \dots \right) \simeq C \ln \frac{2}{\epsilon}. \tag{4}$$

Using (4), (2) becomes

$$V(\zeta) \simeq V \frac{\ln \tan (\zeta/2 + \pi/4)}{\ln (2/\epsilon)}. \tag{5}$$

2.2. *Field along the axis*

We shall now calculate the field at any point M of the tip axis ($\eta=0$), between the tip and the plane. In order to do this, we let η be zero in equation (3), which now reads

$$E(\zeta, 0) = \frac{C}{a \cos^2 \zeta} \tag{6}$$

and, since $x = a \sin \zeta$ if $\eta = 0$,

$$E(x) = \frac{aC}{a^2 - x^2}. \tag{7}$$

We now consider figure 1. The abscissa of the tip apex S is

$$x_S = a \sin \zeta_S = a \cos \epsilon \simeq a \left(1 - \frac{\epsilon^2}{2} \right) \tag{8}$$

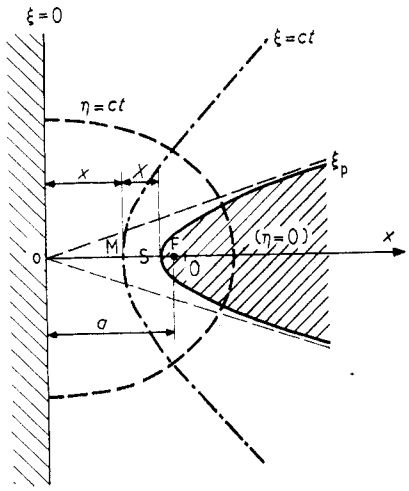

Figure 1. Representation of a point–plane configuration with the various quantities involved. Note that $x+X+r/2=a$ or $u+v+\rho=1$.

and the distance X between point M and the tip apex is

$$X=x_S-x\simeq a\left(1-\frac{\epsilon^2}{2}\right)-x. \tag{9}$$

$$E(X)=\frac{aC}{(X+a\,\epsilon^2/2)\,(2a-X-a\,\epsilon^2/2)}. \tag{10}$$

Expanding the denominator to the second power in ϵ, $E(X)$ reduces to

$$E(X)\simeq\frac{aC}{X(2a-X)+(a-X)\,a\epsilon^2}. \tag{11}$$

Now, it can be easily seen, for instance by expanding the equations of the hyperbola and that of a circle of radius r around the common apex $x=x_S=a\cos\epsilon$ and identifying both expansions, that the radius of curvature of the hyperbola is

$$r=a\frac{\cos^2\zeta}{\sin\zeta}=a\frac{\sin^2\epsilon}{\cos\epsilon}=a\epsilon^2\left(1+\frac{\epsilon^2}{6}+\ldots\right). \tag{12}$$

On the other hand, some algebraic manipulation shows that

$$C=V/\ln\left\{2\left(\frac{a}{r}\right)^{1/2}\left(1+\alpha\frac{r^2}{a^2}-\ldots\right)\right\} \tag{13}$$

where α is a numerical coefficient much smaller than unity. (Note the absence of linear terms in the expansion.) Therefore, to a very good approximation, even if the tip is not very sharp,

$$E(X)=\frac{aC}{X(2a-X)+(a-X)\,r} \tag{14}$$

with

$$C=\frac{V}{\ln\{2(a/r)^{1/2}\}}. \tag{15}$$

In particular, at the tip ($X=0$)

$$E(0)=\frac{C}{r} \tag{16}$$

and at the plane ($X=a-r/2$)

$$E_p=\frac{C}{a}. \tag{17}$$

Numerical application. The factor C is V/k, with $k=\ln\{2(a/r)^{1/2}\}$, and the variation of k with a/r is represented in figure 2, from which it appears that k is close to 5 for typical values of a/r.

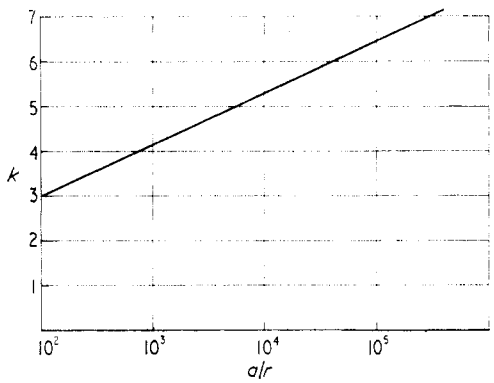

Figure 2. Representation of $k=V/C$ (see text) against $a/r=1/2\rho$.

2.3. *Field on the tip in the vicinity of the tip apex*

On the tip $\zeta=\pi/2-\epsilon$, with $\epsilon\ll 1$, and since, in the vicinity of the apex, $x\simeq x_S\simeq a$, $\eta\ll 1$ in this area.

Hence equation (3) giving the magnitude of the field becomes

$$E(\eta)\simeq\frac{C}{a\epsilon(\epsilon^2+\eta^2)^{1/2}} \tag{18}$$

or

$$E(\eta)\simeq E_0\frac{\epsilon}{(\epsilon^2+\eta^2)^{1/2}} \tag{19}$$

where E_0 is the value of the field at the apex ($\eta=0$).

It is now possible to calculate the area $A(E)$ of the tip surface where the field is higher than a given value $E<E_0$. To do this, we consider the element of tip of area

$$\mathrm{d}A=\frac{2\pi y\,\mathrm{d}x}{\cos\theta} \tag{20}$$

with

$$\tan\theta=\frac{\mathrm{d}y}{\mathrm{d}x} \tag{21}$$

$$\mathrm{d}x\simeq a\eta\,\mathrm{d}\eta \tag{22}$$

$$\mathrm{d}y\simeq a\epsilon\,\mathrm{d}\eta. \tag{23}$$

Using the above relations, $\mathrm{d}A$ becomes

$$\mathrm{d}A=2\pi a^2\epsilon\eta(\epsilon^2+\eta^2)^{1/2}\,\mathrm{d}\eta \tag{24}$$

so that

$$A=2\pi a^2\epsilon\int_0^{\eta}\eta(\epsilon^2+\eta^2)^{1/2}\,\mathrm{d}\eta \tag{25}$$

or

$$A=\frac{2\pi a^2\epsilon}{3}\{(\epsilon^2+\eta^2)^{3/2}-\epsilon^3\}. \tag{26}$$

Introducing equation (19) in the first term of the brace of (26), we obtain

$$A(E)=\tfrac{2}{3}\pi a^2\epsilon^4\left(\frac{E_0^3}{E^3}-1\right) \tag{27}$$

or

$$A(E)=\tfrac{2}{3}\pi r^2\left(\frac{E_0^3}{E^3}-1\right). \tag{28}$$

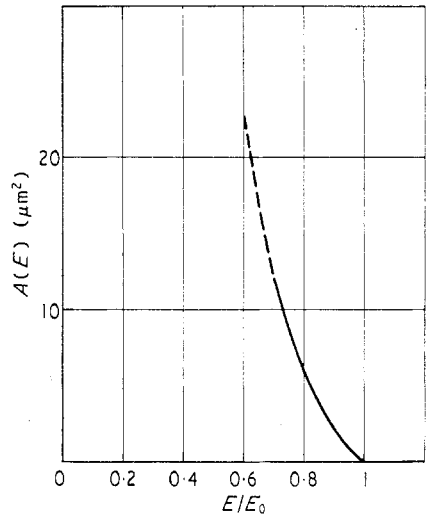

Figure 3. Variation of the area $A(E)$ where the field is higher than $E<E_0$ (apex field) for $r=1$ μm.

3. Transfer time from tip to plane

3.1. *Free carriers*

Suppose that a carrier of mass m and charge q is free to move along the axis in the field calculated above (§2.2). Its dynamical equation is

$$m\ddot{X}=qE(X). \tag{29}$$

If we assume that the carrier starts at rest from the apex ($X=0$), the transfer time, according to the value of $E(X)$ given by (14), can be written as

$$T=a\left(\frac{m\ln(2/\rho)(1+\rho^2)^{1/2}}{2qV}\right)^{1/2}\int_0^{1-\rho}\left(\ln\frac{\phi(v,\rho)}{\phi(0,\rho)}\right)^{-1/2}\mathrm{d}v \tag{30}$$

where

$$\phi(v,\rho)=\frac{(1+\rho^2)^{1/2}-1+\rho+v}{(1+\rho^2)^{1/2}+1-\rho-v} \tag{31}$$

$$v=\frac{X}{a}\qquad\text{and}\qquad\rho=\frac{r}{2a}. \tag{32}$$

The integrand in (30) diverges for $v \to 0$ at the tip apex. However, it is easily seen that, to the first-order approximation in the expansion in terms of v,

$$\ln \frac{\phi(v, \rho)}{\phi(0, \rho)} = \frac{v}{\rho}(1+\rho^2)^{1/2}. \tag{33}$$

Therefore the integral in (30) behaves, in the neighbourhood of $v=0$, as

$$\int_0^v \left(\frac{v}{\rho}(1+\rho^2)^{1/2}\right)^{-1/2} \mathrm{d}v = \frac{2\sqrt{v}}{\{\rho^2(1+\rho^2)\}^{1/4}} \tag{34}$$

and consequently the integral in (30) can be separated as follows:

$$J = \int_0^{1-\rho} [\ldots]^{-1/2}\, \mathrm{d}v = J_1 + J_2 \tag{35}$$

with

$$J_1 = \int_0^{v \ll 1} [\ldots]^{-1/2}\, \mathrm{d}v = \frac{2\sqrt{v}}{\{\rho^2(1+\rho^2)\}^{1/4}} \tag{36}$$

and

$$J_2 = \int_v^{1-\rho} [\ldots]^{-1/2}\, \mathrm{d}v. \tag{37}$$

J_2 can be evaluated with a digital computer. We have chosen $v = 10^{-2}\rho$, but we have verified that the final result is independent of the choice of v—provided that $v \ll 1$—within the accuracy of the calculation.

The results are presented below for $a = 1$ cm and $V = 10^3$ V.

Table 1. Transfer times *in vacuo* for electrons and singly charged ions of mass $M=16$ without initial velocity, for $a=1$ cm and $V=1$ kV

ρ	$a\left(\frac{m \ln (2/\rho)\,(1+\rho^2)^{1/2}}{2qV}\right)^{1/2}$	J	T(el) (s)	T(ion) $= 171\ T$(el) (s)
$0{\cdot}5\times10^{-3}$	$1{\cdot}61\times10^{-9}$	0·386	$6{\cdot}2\times10^{-10}$	$1{\cdot}06\times10^{-7}$
$0{\cdot}5\times10^{-4}$	$1{\cdot}82\times10^{-9}$	0·332	$6{\cdot}05\times10^{-10}$	$1{\cdot}03\times10^{-7}$
$0{\cdot}5\times10^{-5}$	$2{\cdot}01\times10^{-9}$	0·296	$5{\cdot}95\times10^{-10}$	$1{\cdot}02\times10^{-7}$

3.2. *Bound carriers moving along a field line off the axis*

We now assume that the carrier moves with the mobility μ along a field line defined by the parameter η. Its position on this line is defined by ζ, and its motion obeys the equation

$$\frac{\mathrm{d}s}{\mathrm{d}t} = -\mu E_\zeta$$

where

$$\mathrm{d}s = (\mathrm{d}x^2 + \mathrm{d}y^2)^{1/2} = a(\cosh^2\eta - \sin^2\zeta)^{1/2}\, \mathrm{d}\zeta. \tag{38}$$

Hence

$$\mathrm{d}t = -\frac{a(\cosh^2\eta - \sin^2\zeta)^{1/2}}{\mu E}\, \mathrm{d}\zeta \tag{39}$$

or, using (3),

$$\mathrm{d}t = -\frac{a^2}{\mu C}\cos\zeta(\cosh^2\eta - \sin^2\zeta)\, \mathrm{d}\zeta. \tag{40}$$

Hence the transit time from the point ($\zeta=\pi/2-\epsilon$) to the plane ($\zeta=0$) is

$$T=-\frac{a^2}{\mu C}\int_{\pi/2-\epsilon}^{0}\cos\zeta(\cosh^2\eta-\sin^2\zeta)\,\mathrm{d}\zeta \tag{41}$$

or

$$T=\frac{a^2}{\mu C}\cos\epsilon\left(\cosh^2\eta-\frac{\cos^2\epsilon}{3}\right)\simeq\frac{a^2}{\mu C}(\cosh^2\eta-\tfrac{1}{3}). \tag{42}$$

For $\eta=0$ (axis), one finds the simple result $T_0=2a^2/3\mu C$.

Numerical application. If we assume $a=1$ cm with $a/r=10^4$, $\mu=10^{-3}$ cm^2 V^{-1} s^{-1} and $V=10^4$ V, we find $T_0=0{\cdot}35$ s.

4. Induced current

In order to find the current induced in the external circuit by charges moving within the electrode gap, we first assume that the charges are positive and we further assume that the tip and the plane form a total influence capacitor. We then apply the principle of superposition to the system described below:

	Charges			Potentials		
	Charge	Tip	Plane	Charge	Tip	Plane
1st configuration	q	Q_1	Q_2	V_M	0	0
2nd configuration	0	Q'_1	Q'_2	V'_M	V'_1	V'_2

Q_1 and Q_2 are the negative charges induced on the tip and plane respectively, assumed at potential 0, by the charge q at M where the potential is V_M. In the second configuration, the charges Q' and potentials are defined in the same manner but in the absence of the moving charge, so that $V'_M=V(\zeta)$.

Since all tubes of flux at M reach both electrodes,

$$q+Q_1+Q_2=0. \tag{43}$$

Furthermore, if Green's reciprocation theorem is applied for configurations 1 and 2,

$$qV'_M+Q_1V'_1+Q_2V'_2=0. \tag{44}$$

Combining (43) and (44) gives Q_1 and Q_2:

$$Q_{1,2}=-\frac{V'_M-V'_{2,1}}{V'_{1,2}-V'_{2,1}}q. \tag{45}$$

In our problem V'_2 is the potential of the tip with respect to that of the plane ($V'_1=0$). Hence the charge Q_1 induced on the plane in configuration 1 is

$$Q_1=\frac{V(\zeta)-V}{V}q. \tag{46}$$

The current induced in the external circuit by the charge q moving on its flux lines is given by the rate of change of Q_1:

$$i=-\frac{\mathrm{d}Q_1}{\mathrm{d}t}=-\frac{q}{V}\frac{\mathrm{d}V(\zeta)}{\mathrm{d}t} \tag{47}$$

or

$$i=-\frac{q}{V}\frac{\partial V(\zeta)}{\partial\zeta}\frac{\zeta}{\partial s}\frac{\mathrm{d}s}{\mathrm{d}t}. \tag{48}$$

From (2)

$$\frac{\partial V(\zeta)}{\partial \zeta}=\frac{C}{\cos\zeta}. \tag{49}$$

From (23)

$$\frac{\partial \zeta}{\partial s}=\frac{1}{a(\cosh^2\eta-\sin^2\zeta)^{1/2}} \tag{50}$$

and from (3)

$$\frac{\mathrm{d}s}{\mathrm{d}t}=-\mu E=\frac{-\mu C}{a\cos\zeta(\cosh^2\eta-\sin^2\zeta)^{1/2}}. \tag{51}$$

Finally

$$\boxed{i(\zeta,\eta)=\frac{q}{V}\frac{\mu C^2}{a^2\cos^2\zeta(\cosh^2\eta-\sin^2\zeta)}}. \tag{52}$$

In order to relate i to the time t after the charge q has left the tip, we must go back to equation (40) which, integrated from the tip ($\zeta=\pi/2-\epsilon$) to a point of parameter $\zeta\neq 0$, gives

$$t(\zeta,\eta)=-\frac{a^2}{\mu C}\int_{\pi/2-\epsilon}^{\zeta}\cos\zeta\,(\cosh^2\eta-\sin^2\zeta)\,\mathrm{d}\zeta \tag{53}$$

or

$$t(\zeta,\eta)=-\frac{a^2}{\mu C}\left\{\sin\zeta\left(\cosh^2\eta-\frac{\sin^2\zeta}{3}\right)-\cos\epsilon\left(\cosh^2\eta-\frac{\cos^2\epsilon}{3}\right)\right\} \tag{54}$$

that is

$$\boxed{t(\zeta,\eta)\simeq\frac{a^2}{3\mu C}(1-\sin\zeta)\,(3\cosh^2\eta-1-\sin\zeta-\sin^2\zeta).} \tag{55}$$

Finally, $i(t)$ is defined, for a given flux line η, by the parametric equations (52) and (55), from which the set of curves of figure 4, corresponding to values of sinh η between 0 (tip axis) and 1, has been obtained.

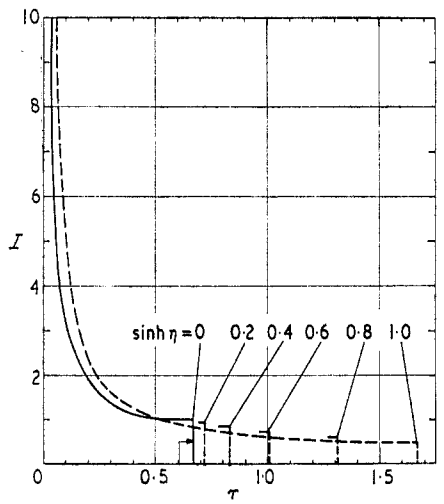

Figure 4. Variation of $I=(a^2V/q\mu C^2)\,i(\xi,\eta)$ against $\tau=(\mu C/a^2)\,t(\xi,\eta)$ (cf. text, equations (52) and (55)). Full curve: sinh $\eta=0$ (on axis). Broken curves: sinh $\eta>0$ (off axis). For $0<\sinh\eta<1$, only partial curves have been drawn for clarity.

Single prebreakdown current transients can be observed with a tip–plane electrode configuration immersed in liquid dielectrics such as liquid nitrogen (Coelho and Sibillot 1970 a), when the applied voltage is carefully adjusted to the prebreakdown threshold level. Such a transient, shown in figure 5, results from the motion from tip to plane of charge released by a single breakdown event.

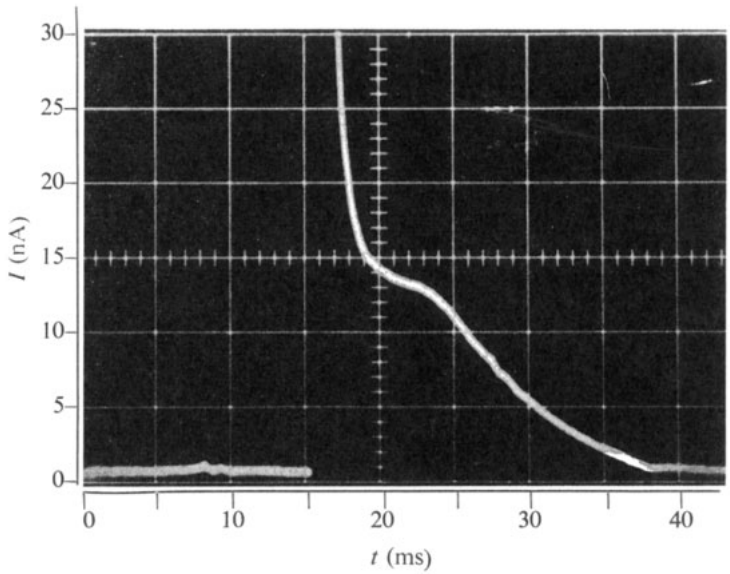

Figure 5. Experimental recording of a single current pulse in liquid nitrogen, presumably due to the motion of a diffuse charge from the point to the plane ($V=15$ kV, $d=0{\cdot}34$ cm).

As suggested from optical observations (Farazmand 1968, Chadband and Wright 1965), a prebreakdown event generates charge carriers with momentum in all directions about the tip axis, and the actual transient of figure 5 might possibly be regarded as a properly weighted summation, over a wide range of η, of transients such as those shown in figure 4. Conversely, an analysis of actual transients in terms of the elementary transients might prove worthwhile in breakdown studies.

5. Space-charge distortion

Up to this point, it was assumed that the space between the point and the plane is free of charge, so that the field is identical to the 'geometric' field given by Laplace's equation.

We now drop this restricting assumption and consider the steady-state situation occurring when the tip emits charges of mobility μ into a condensed phase of permittivity ϵ.

The sign of the emitted charges is assumed to be that of the tip, the mobility μ is assumed to be independent of the field strength and the diffusion current is assumed to be negligible with respect to the conduction current.

5.1. *Derivation and solution of the self-consistent field equation*

Under these conditions, the current density at any point of the gap is given by

$$\boldsymbol{j}=ne\mu\boldsymbol{E} \tag{56}$$

where ne is related to the field by Poisson's equation

$$ne=\epsilon\nabla.\boldsymbol{E}. \tag{57}$$

Relations (56) and (57) combine to give

$$\boldsymbol{j}=\mu\epsilon(\boldsymbol{\nabla}.\boldsymbol{E})\,\boldsymbol{E} \tag{58}$$

and, in the steady state, we have

$$\boldsymbol{\nabla}.\boldsymbol{j}=\mu\epsilon\boldsymbol{\nabla}.\{(\boldsymbol{\nabla}.\boldsymbol{E})\,\boldsymbol{E}\}=0 \tag{59}$$

or

$$(\boldsymbol{\nabla}.\boldsymbol{E})^2+\boldsymbol{E}.\boldsymbol{\nabla}(\boldsymbol{\nabla}.\boldsymbol{E})=0. \tag{60}$$

Owing to the presence of space charge, the hyperboloids defined by (1) are no longer equipotential surfaces. It is, however, advisable to keep the same coordinate system, or, more precisely, the three-dimensional system deduced from (1) by the transformation

$$\begin{aligned} x' &= -y\sin\psi=-a\sinh\eta\cos\zeta\sin\psi \\ y' &= -y\cos\psi=-a\sinh\eta\cos\zeta\cos\psi \\ z' &= x=a\cosh\eta\sin\zeta \end{aligned} \tag{61}$$

where ψ is the polar angle with respect to the z' axis. Under these conditions, the divergence of a vector $\boldsymbol{E}$ for a configuration possessing symmetry of revolution around z' is (Angot 1953)

$$\boldsymbol{\nabla}.\boldsymbol{E}=\frac{1}{a\Delta^3}\left(\frac{2\sinh^2\eta+\cos^2\zeta}{\tanh\eta}E_\eta-\frac{2\cos^2\zeta+\sinh^2\eta}{\cot\zeta}E_\zeta\right)+\frac{1}{a\Delta}\left(\frac{\partial E_\eta}{\partial\eta}+\frac{\partial E_\zeta}{\partial\zeta}\right) \tag{62}$$

where

$$\Delta=(\cosh^2\eta-\sin^2\zeta)^{1/2}. \tag{63}$$

The problem of finding the general solution of (60), in which $\boldsymbol{\nabla}.\boldsymbol{E}$ has the value given above, is obviously of inextricable complexity.

However, the problem is considerably simplified if we forget our attempt to calculate the field at any point and restrict our ambition to the calculation of the field on the tip axis, where $\eta=0$. Since E_η is an even function of η such as $E_0=0$, the expansion of E_η for small values of η is of the form $E_\eta=\alpha\eta^2+\beta\eta^4+\ldots$ and consequently

$$\lim_{\eta\to0}\frac{E_\eta}{\tanh\eta}=\lim_{\eta\to0}\frac{\mathrm{d}E_\eta}{\mathrm{d}\eta}=0 \tag{64}$$

and, since $\Delta_{\eta=0}=\cos\zeta$,

$$(\boldsymbol{\nabla}.\boldsymbol{E})_{\eta=0}=-\frac{2\sin\zeta}{a\cos^2\zeta}E_\zeta+\frac{1}{a\cos\zeta}\frac{\partial E_\zeta}{\partial\zeta}. \tag{65}$$

The gradient of this quantity, which is directed along the axis, takes the simple form

$$\boldsymbol{\nabla}(\boldsymbol{\nabla}.\boldsymbol{E})=\frac{1}{a\cos\zeta}\frac{\zeta}{\partial\zeta}\left\{\frac{1}{a\cos\zeta}\left(\frac{\partial E_\zeta}{\partial\zeta}-2\tan\zeta E_\zeta\right)\right\}. \tag{66}$$

After deriving from (66) the expressions for $\boldsymbol{E}.\boldsymbol{\nabla}(\boldsymbol{\nabla}.\boldsymbol{E})$ and $(\boldsymbol{\nabla}.\boldsymbol{E})^2$ on the axis and introducing these expressions in (60), the latter becomes

$$\frac{\mathrm{d}^2E^2}{\mathrm{d}\zeta^2}-5\tan\zeta\frac{\mathrm{d}E^2}{\mathrm{d}\zeta}-4E^2=0. \tag{67}$$

Since ζ is the only variable of our problem, the partial derivatives $\partial/\partial\zeta$ have been replaced here by total derivatives and the index ζ is dropped for convenience.

By letting $Y=E^2\cos^4\zeta$, the second-order differential equation (67) can be converted into the equation

$$\frac{\mathrm{d}^2Y}{\mathrm{d}\zeta^2}+3\tan\zeta\frac{\mathrm{d}Y}{\mathrm{d}\zeta}=0 \tag{68}$$

where the term of order zero has disappeared.

Integration of equation (68) is straightforward:

$$\frac{dY}{d\zeta}=A\cos^3\zeta \tag{69}$$

so that

$$Y=A\left(\sin\zeta-\frac{\sin^3\zeta}{3}\right)+B \tag{70}$$

where A and B are the constants of integration.

Finally, one obtains for E the expression

$$E_\zeta=\frac{1}{\cos^2\zeta}\left\{A\left(\sin\zeta-\frac{\sin^3\zeta}{3}\right)+B\right\}^{1/2} \tag{71}$$

or, using (1) and letting u be x/a,

$$E(u)=\frac{\{Au(1-u^2/3)+B\}^{1/2}}{1-u^2}. \tag{72}$$

Remarks. (*a*) Relation (71) should be compared with the relation $E=B'/\cos^2\zeta$ obtained in the absence of space charge. (*b*) The constant A is negative, since the magnitude of E when space charge is present is smaller, close to the emitter, than in the absence of space charge.

A relation between A and B is obtained by writing that the voltage drop between the electrodes is V:

$$\int_0^{1-\rho}E(u)\,du=\frac{V}{a}. \tag{73}$$

5.2. *Significance of the integration constants*

5.2.1. *Significance of A.* Introducing (71) into relation (58) to give the current density j yields

$$j=\frac{\mu\epsilon}{2a\cos^2\zeta}\left(\frac{dE^2}{d\zeta}\cos\zeta-4E_\zeta\sin\zeta\right) \tag{74}$$

with

$$E^2\cos^4\zeta=A\left(\sin\zeta-\frac{\sin^3\zeta}{3}\right)+B. \tag{75}$$

Differentiating (75) gives

$$\frac{dE_\zeta^2}{d\zeta}\cos^4\zeta-4E_\zeta^2\sin\zeta=A. \tag{76}$$

Consequently

$$j(\zeta)=\frac{\mu\epsilon A}{2a\cos^2\zeta}. \tag{77}$$

In particular, at the plane ($\zeta=0$),

$$j_0=\frac{\mu\epsilon A}{2a}. \tag{78}$$

Relation between A and the total emitted current. Even under the unrealistic assumptions that (*a*) the space-charge-limited current off the axis could be obtained analytically and (*b*) the plane electrode is of infinite radius, one must keep in mind that most of the current is injected from the tip, where the field is a maximum, since all charge injection processes such as Schottky or field emission depend sharply on the field.

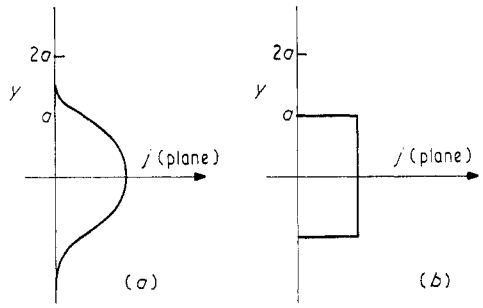

Figure 6. Hypothetical current density distribution on the plane and its simplified approximation (cf. equation (79)). (*a*) Actual j distribution. (*b*) Assumed j distribution.

Accordingly, the current density on the plane, vanishing rapidly with increasing distance from the tip axis, is sketched in figure 6(*a*). The tip–plane distance being very close to a, the area of the plane at a distance less than a from the axis is seen from the tip as the angle $\pi/4$ rad (solid angle $0{\cdot}6\pi$ sr) compatible with the experimental conditions.

In view of the insoluble uncertainty in the actual current density profile, the latter can be roughly approximated as that of figure 6(*b*). This approximation relates A to the emitted current I by

$$I=\pi a^2 j_0=\frac{\pi}{2}\, a\epsilon\mu A.$$

Hence

$$A=\frac{2I}{\pi a\epsilon\mu}. \tag{79}$$

5.2.2. *Significance of B.* B can be related to the value of E at the tip apex as follows. Equation (72) can be rewritten as

$$(1-u^2)^2\, E^2=Au\left(1-\frac{u^2}{3}\right)+B \tag{80}$$

and, at the point apex ($u=u_\mathrm{p}$), (80) takes the form

$$(1-u_\mathrm{p}^2)^2\, E_\mathrm{p}^2=Au_\mathrm{p}\left(1-\frac{u_\mathrm{p}^2}{3}\right)+B \tag{81}$$

where u_p and E_p are the values of u and E at the point apex ($v=0$).

Elimination of B between (80) and (81) gives

$$(1-u^2)^2\, E^2=(1-u_\mathrm{p}^2)^2\, E_\mathrm{p}^2-\frac{A}{3}\,(u_\mathrm{p}-u)\,(3-u_\mathrm{p}^2-u_\mathrm{p}u-u^2) \tag{82}$$

or, coming back to the variable v, we can write E in the form

$$E(v)=\frac{[\rho^2(2-\rho)^2E_\mathrm{p}^2-Av\{\rho(2-\rho)+(1-\rho)\,v-v^2/3\}]^{1/2}}{(v+\rho)\,(2-v-\rho)} \tag{83}$$

and relation (73) becomes

$$\int_0^{1-\rho} E(v)\,\mathrm{d}v=-\frac{V}{a}. \tag{84}$$

5.3. *Integration of $E(v)$*

In order to integrate (83) conveniently, the domain of integration can be divided into the vicinity of the apex ($v\simeq 0$) on the one hand, and the rest of the domain.

In the vicinity of the apex, the second term in the brace of (83) is negligible with respect to the first, so that

$$E(v) \simeq \frac{\rho(2-\rho)\, E_p}{(v+\rho)\,(2-v-\rho)} \tag{85}$$

and

$$\int_0^{v\simeq 0} E(v)\, dv = \frac{1}{a}\,(V - V(v)) = \frac{\rho(2-\rho)}{2} E_p \ln \frac{1+v/\rho}{1-v/(2-\rho)}. \tag{86}$$

By expanding the logarithm of (86) in terms of increasing powers of v, accounting for the fact that $\rho \ll 1$, and coming back to the variable X, it appears that, in the vicinity of the apex,

$$V - V(X) = E_p \left(X + \frac{X^2}{r} + \ldots \right)$$

which shows that the voltage deviates very quickly from linearity near the tip apex.

On the other hand, if the current is space-charge limited, the emitter field vanishes, so that

$$E(v) = (-A)^{1/2} \frac{[\{\rho(2-\rho) + (1-\rho)\, v - v^2/3\}\, v]^{1/2}}{(\rho+v)\,(2-\rho-v)} \tag{87}$$

and analytic integration of $E(v)$ is possible if ρ is neglected with respect to unity. Under this assumption,

$$-\frac{V}{a} = (-A)^{1/2} \int_0^1 \frac{(1-v/3)^{1/2}}{2-v}\, dv = \left(-\frac{A}{3}\right)^{1/2} \int_1^2 \frac{(1+w)^{1/2}}{w}\, dw \tag{88}$$

or

$$-\frac{V}{a} = \left(-\frac{A}{3}\right)^{1/2} \left| 2(1+w)^{1/2} + \ln \frac{(1+w)^{1/2}-1}{(1+w)^{1/2}+1} \right|_1^2 = 0{\cdot}624(-A)^{1/2}. \tag{89}$$

5.4. *Graphical representation*

Figure 7 represents the variation of $(-A)^{1/2}$ against V for various values of E_p. The voltage drop V as defined by the integral

$$\int_0^{1-\rho} E(v, A)\, dv$$

has been calculated in the following way. The domain of the variable v has been divided into two subdomains (0–0·01) and (0·01–ρ).

The integration was performed analytically in the first domain according to equation (86) and numerically in the second one.

All the curves are asymptotic to the straight line of the equation $(-A)^{1/2} = V/0{\cdot}624a$. From the $(\sqrt{I}, V)$ characteristics it is possible to deduce the mobility of the injected carriers, under the reasonable simplifying assumption that the slope of the curve is identical with that of the straight line.

The family of curves $(-A)^{1/2} = f(V, r)$ for given E_p can be deduced from figure (8) by noting that V varies slowly with r for a given value of $rE_p = k$. Hence figure 8 represents roughly the curves

$$(-A)^{1/2} = f(V, k = rE_p)$$

from which the curves $(-A)^{1/2} = f(v, r)|_{E_p = \text{constant}}$ can be obtained.

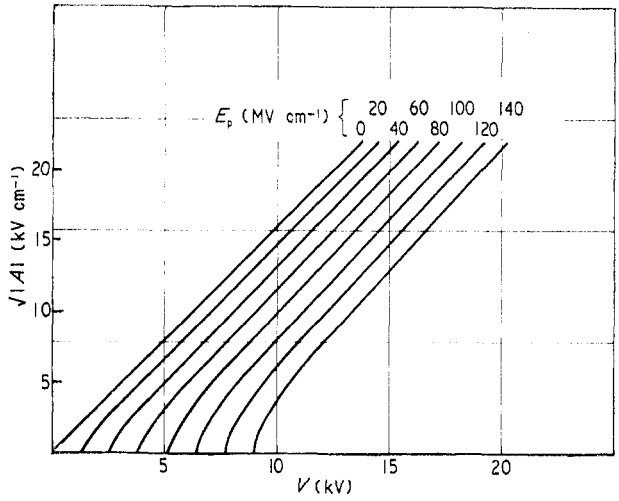

Figure 7. $(-A)^{1/2}$ against V for various values of E_p (apex field) with $r=0{\cdot}1$ μm and $a=1$ cm.

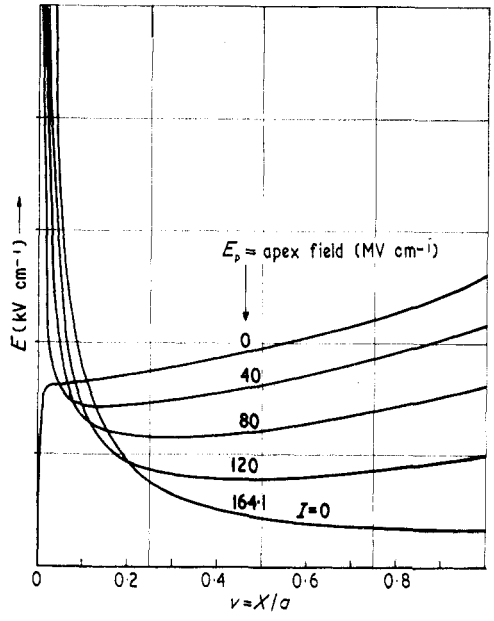

Figure 8. Field distribution along the axis from the apex ($v=0$) to the plane ($v=1-\rho$) for various values of E_p between $E_p=0$ (complete space-charge limitation) and $E_p=164$ MV cm^{-1} (no space charge, $I=0$) for $V=10$ kV, $r=0{\cdot}1$ μm and $a=1$ cm.

The value of the totally space-charge-limited current, as obtained from (79) and (89), is

$$I=\frac{\pi}{0{\cdot}78}\,\epsilon\mu\,\frac{V^2}{a} \tag{90}$$

and it is worth comparing this relation with that obtained in spherical geometry (Coelho and Sibillot 1970) with the same injection solid angle $\Omega=0{\cdot}6\pi$:

$$I_s=\frac{\pi}{4{\cdot}45}\,\epsilon\mu\,\frac{V^2}{a}. \tag{91}$$

This gives $I/I_s=5{\cdot}7$.

Finally, the curves $E(v)$ for various values of the current I, from $I=0$ (no space charge) to the maximum value given by (90) for complete space-charge limitation, are represented in figure 8. The general shape of the curves agrees with that predicted by Atten (1970).

6. Conclusion

For a point–plane electrode configuration approximated by a hyperboloid plan system, most of the characteristic properties of practical importance to the engineer (field distribution, transfer times, etc.) have been analysed.

In particular, straightforward assumptions permit the prediction of the variation of the partially space-charge-limited current with the applied voltage and the derivation from the current–voltage characteristics of a rough determination of the mobility of the injected charge carriers.

References

ANGOT, A., 1953, *Complément de Mathématiques, 3ème edition, Editions de la Revue d'Optique, Paris.*

ATTEN, P., 1970, *Thesis*, Grenoble.

CHADBAND, W. G., and WRIGHT, G. T., 1965, *Br. J. appl. Phys.*, **16**, 305.

COELHO, R., and SIBILLOT, P., 1970 a, *Revue gén. Elect.*, **79**, 29.

—— 1970 b, *IEE Conf. on Dielectric Materials, Lancaster, IEE Conf. Publ. No.* 67, p. 105.

DRECHSLER, M., and HENKEL, O., 1964, *Z. angew. Phys.*, **61**, 341.

DURAND, E., 1966, *Electrostatique* (Paris: Masson).

FARAZMAND, B., 1961, *Br. J. appl. Phys.*, **12**, 251.

GOMER, R., 1961, *Field Emission and Field Ionization* (Harvard: Harvard University Press).

NIKOLOPOULOS, P., 1966, *Elektrotech. Z. A.*, **87**, 239.